Interannual Variability in the Pathways of the North Atlantic Current over the Mid-Atlantic Ridge and the Impact of Topography

AMY S. BOWER

Department of Physical Oceanography, Woods Hole Oceanographic Institution, Woods Hole, Massachusetts

WILKEN-JON VON APPEN

Department of Physical Oceanography, Woods Hole Oceanographic Institution, Woods Hole, Massachusetts, and Jacobs University Bremen, Bremen, Germany

(Manuscript received 28 August 2006, in final form 23 February 2007)

ABSTRACT

Recent studies have indicated that the North Atlantic Ocean subpolar gyre circulation undergoes significant interannual-to-decadal changes in response to variability in atmospheric forcing. There are also observations, however, suggesting that the southern limb of the subpolar gyre, namely, the eastward-flowing North Atlantic Current (NAC), may be quasi-locked to particular latitudes in the central North Atlantic by fracture zones (gaps) in the Mid-Atlantic Ridge. This could constrain the current's ability to respond to variability in forcing. In the present study, subsurface float trajectories at 100–1000 m collected during 1997–99 and satellite-derived surface geostrophic velocities from 1992 to 2006 are used to provide an improved description of the detailed pathways of the NAC over the ridge and their relationship to bathymetry. Both the float and satellite observations indicate that in 1997–99, the northern branch of the NAC was split into two branches as it crossed the ridge, one quasi-locked to the Charlie–Gibbs Fracture Zone (CGFZ; 52°–53°N) and the other to the Faraday Fracture Zone (50°–51°N). The longer satellite time series shows, however, that this pattern did not persist outside the float sampling period and that other branching modes persisted for one or more years, including an approximately 12-month time period in 2002–03 when the strongest eastward flow over the ridge was at ~49°N. Schott et al. showed how northward excursions of the NAC can temporarily block the westward flow of the Iceland–Scotland Overflow Water through the CGFZ. From the 13-yr time series of surface geostrophic velocity, it is estimated that such blocking may occur on average 6% of the time, although estimates for any given 12-month period range from 0% to 35%.

1. Introduction

The Gulf Stream and its northeastward extension, the North Atlantic Current (NAC), are the primary conduits by which warm waters are transported from the tropics to high latitudes, where they are cooled and transformed into cold deep waters that fill much of the world's ocean basins. The NAC flows northward along the western boundary east of the Grand Banks as far as about 52°N where it makes a large anticyclonic meander, called the Northwest Corner (Worthington 1976), and turns eastward toward the Mid-Atlantic Ridge (MAR) [see Rossby (1996), for a review and Fig. 1a for a schematic representation].

Most of what is known about the eastward-flowing NAC has been learned from hydrographic sections and surface drifters; satellite infrared imagery is of little use here due to persistent cloudiness. From these observations, it has been determined that the NAC does not cross the North Atlantic Ocean as a broad eastward drift nor a single, well-defined current like the Gulf Stream. Rather it consists of from two to four narrow (~100 km wide) branches with mean surface velocity of ~0.2 m s^{-1} that meander across the North Atlantic in the latitudinal band 45°–53°N (Krauss 1986; Sy 1988; Sy et al. 1992; Belkin and Levitus 1996). There is some evidence that at least the northern branch of the NAC, also called the Subarctic or Subpolar Front (SPF), is

Corresponding author address: Dr. Amy S. Bower, Woods Hole Oceanographic Institution, MS 21, Woods Hole, MA 02540.
E-mail: abower@whoi.edu

DOI: 10.1175/2007JPO3686.1

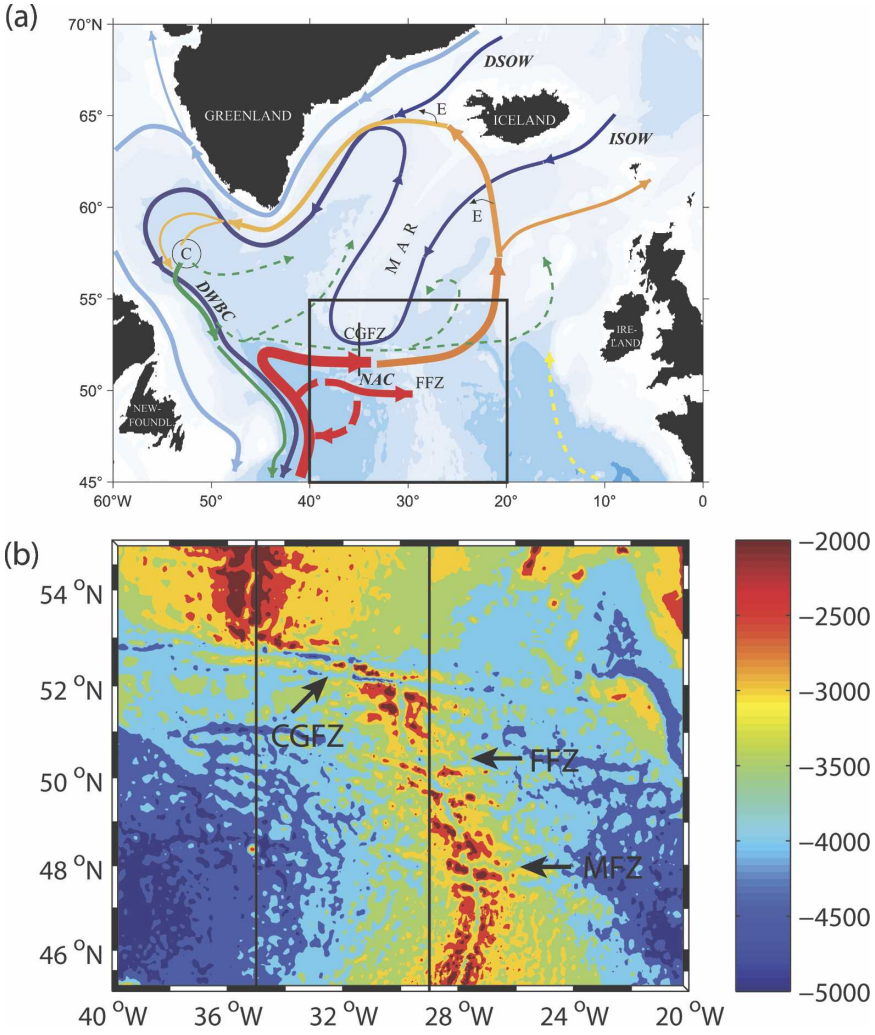

FIG. 1. (a) General circulation patterns at the surface and at depth in the northern North Atlantic (reproduced from Schott et al. 1999). Study area around the Mid-Atlantic Ridge is indicated by the rectangular box. (b) Shaded bathymetry in 500-m intervals in the study area from 45° to 55°N and from 20° to 40°W. Major fracture zones are the CGFZ (52°–53°N), the FFZ (50°–51°N), and the MFZ (48°N) (acronyms are defined in section 1). Bathymetry has 2′ resolution (Smith and Sandwell 1997).

constrained in its latitudinal movement where it flows over the MAR. For example, Sy (1988) and Sy et al. (1992) used several synoptic hydrographic sections and current-meter data from the Topographic Gulf Steam (TOPOGULF) experiment to argue that the northern branch of the NAC typically crosses the ridge over the Charlie–Gibbs Fracture Zone (CGFZ), the widest (100 km) and deepest (>3500 m) gap in the MAR (see Fig. 1b). This is presumably due to the interactions of the deeper NAC currents with the ridge bathymetry, which will tend to steer the currents through deeper passes in the ridge to conserve potential vorticity. These authors concluded that southern branches are less constrained and are found at various latitudes as far south as 45°N. Belkin and Levitus (1996) used repeated Russian hydrographic sections occupied in the years 1976–85 to show that the northern NAC branch exhibits strong interannual variability in its latitude upstream of the ridge crest, but is more confined near the CGFZ.

Other authors have attempted to relate interannual-to-decadal changes in subpolar gyre circulation to variability in wind stress over the North Atlantic, which is often scaled in terms of the North Atlantic Oscillation (NAO) index (e.g., Curry and McCartney 2001; Flatau et al. 2003; Häkkinen and Rhines 2004). Of particular interest here are the studies of variability in NAC pathways and its relationship to changing wind stress patterns. Heywood et al. (1994) and White and Hey-

wood (1995) used up to four years of altimetric data between 1986 and 1994 to show that large-scale, interannual north–south shifts in the NAC system in the central North Atlantic could be correlated with changes in the strength of the wind stress. Bersch et al. (1999) used repeated hydrographic sections between Greenland and Ireland in 1991–96 to show that the eastern limb of the subpolar gyre retreated westward (gyre contraction) during a low phase of the NAO index.

Still not completely answered by these earlier studies is the extent to which the individual NAC branches are dynamically constrained to cross the MAR at the latitudes of the deepest gaps in the ridge. Is the NAC's northern branch *always* confined to the CGFZ? Are the other branches similarly constrained to other gaps? What is the character of the temporal variability in these pathways? These questions have been difficult to address using a limited number of synoptic hydrographic sections, or even a large number of nonsynoptic sections, due to the large-amplitude meandering of the NAC branches upstream and downstream of the MAR (Belkin and Levitus 1996). The questions seem worth pursuing further because of the possible implications for the response of the subpolar gyre to interannual-to-decadal variability in atmospheric forcing, and thus for the delivery of warm water to high latitudes in the North Atlantic. In the present study, we attempt to partially address these questions by tracing the NAC branches continuously over the MAR, thus providing an improved description of their pathways in relation to the detailed bathymetry of the MAR. Specifically, we use high-resolution trajectories from acoustically tracked subsurface floats and satellite altimetric observations of surface geostrophic velocity to document the locations of the NAC branches over the ridge and their temporal variability between 1992 and 2006. This is an extension of an earlier study by Bower et al. (2002), who analyzed the trajectories of the subsurface floats during 1997–99 alone and found that they tended to cross the ridge in several narrow latitudinal bands, one over the CGFZ (52°–53°N), a second over the Faraday Fracture Zone (FFZ; 50°–51°N), and a third over the Maxwell Fracture Zone (MFZ; 48°N). Here we first establish the correspondence of the NAC pathways as independently revealed by the floats and maps of surface geostrophic velocity. We then use the 13-yr time series of surface currents to document interannual variability in NAC pathways over the ridge. In the next section, we describe the datasets used in this study, and the results are presented in section 3. Discussion and conclusions are given in section 4.

2. Data and methods

a. RAFOS floats

In 1997–98, about 85 long-term, isopycnal RAFOS floats (Rossby et al. 1986) were released on three different cruises in and around the NAC branches west of the Mid-Atlantic Ridge by the Woods Hole Oceanographic Institution and the University of Rhode Island to investigate the pathways of the warm water entering the subpolar region. This effort was part of the U.S. contribution to the World Ocean Circulation Experiment (WOCE) and the Atlantic Circulation and Climate Experiment (ACCE). The floats were ballasted for the $27.5\sigma_\theta$ density surface (main thermocline), which varies in depth from 100 to 1000 m across the NAC. They were tracked acoustically using an array of U.S. and European sound sources, resulting in position, temperature, and pressure measurements once per day for 18–24 months. Tracking accuracy was on the order of 5 km. More details on the float dataset can be found in Bower et al. (2002), Furey et al. (2001), and Anderson-Fontana et al. (2001).

b. Satellite altimetry

In this study, we used maps of absolute dynamic topography (MADT) and surface geostrophic velocity produced by Ssalto/Duacs at Collecte Localization Satellites (CLS), a subsidiary of the French Space Agency [the Centre National d'Etudes Spatiales (CNES)] and the French Research Institute for Exploration of the Sea (IFREMER). This product is generated using satellite altimetry data obtained by the Ocean Topography Experiment (TOPEX)/Poseidon (1992–2002), *Jason-1* (2002–06), *European Remote Sensing Satellite-1* (*ERS-1*; 1992–93, 1995) and *-2* (*ERS-2*; 1996–2003), and *Environmental Satellite* (*Envisat*; 2003–06) satellite missions. (With support from CNES it is distributed online by Aviso at http://www.jason.oceanobs.com/html/donnees/produits/hauteurs/global/madt_uk.html.)

Except for January 1994–March 1995 the reference product is constantly based on two satellites. It has been interpolated onto a grid with a ⅓° × ⅓° spatial and a 7-day temporal resolution starting in October 1992. To compute the MADT, CLS Space Oceanography Division combines the sea level anomalies (SLA) measured by the satellites in real time with its Combined Mean Dynamic Topography (Rio05). Rio and Hernandez (2004) and Rio et al. (2006) describe how the Combined Mean Dynamic Topography is constructed. Here we analyze data from 14 October 1992 to 18 January 2006 in the region around the MAR from 45° to 55°N, 20° to 40°W (box in Fig. 1a).

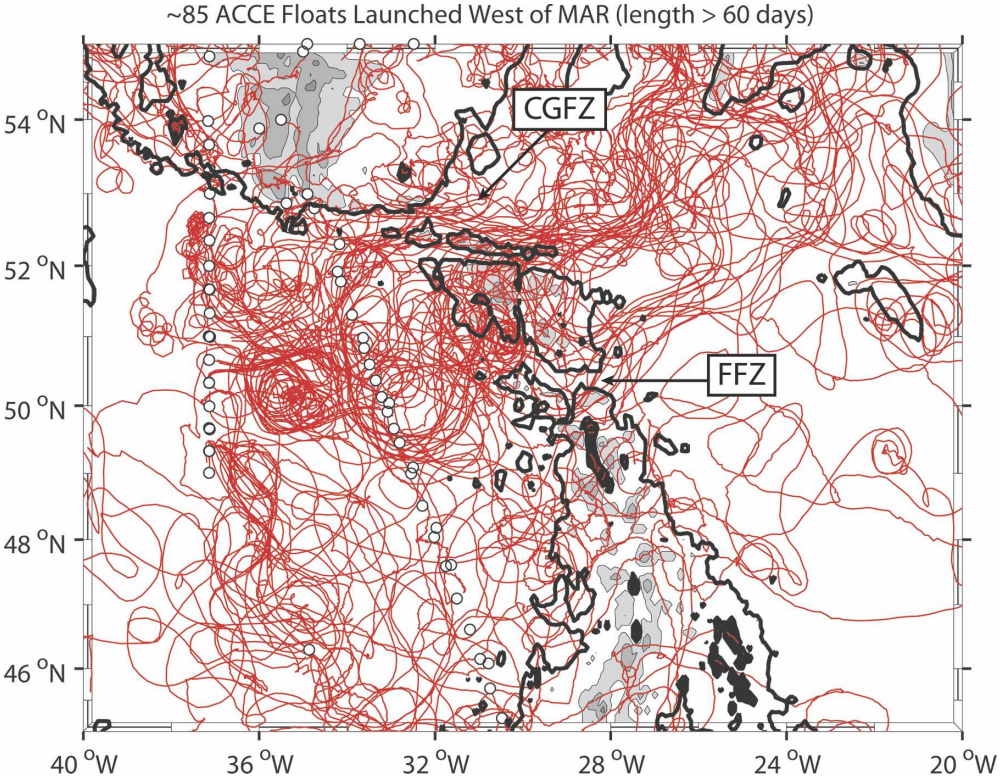

FIG. 2. Trajectories of about 85 acoustically tracked RAFOS floats that were deployed west of the MAR (open circles) in three settings: June 1997, October–November 1997, and July 1998. The floats were ballasted for the 27.5σ_θ potential density surface, which ranges in depth from about 100 to 1000 m across the NAC. The 3000-m isobath is superimposed (heavy black line) to indicate the CGFZ and FFZ.

c. *Bathymetry*

In most of the following figures, we have used the 2′ gridded bathymetry of Smith and Sandwell (1997) to illustrate the features of the MAR (Fig. 1b). North of 53°N and south of 47.5°N the ridge is relatively "solid" and shallow, being everywhere less than 2500 m. Between these two higher segments, the ridge is considerably fractured and has several deep gaps. The three deepest quasi-zonal gaps completely across the ridge are the CGFZ, FFZ, and MFZ. In some areas, the central rift valley is also quite deep (>3000 m). It provides a deep connection between the CGFZ and FFZ. At 2500 m, there are numerous smaller gaps in the eastern and western flanks of the ridge, giving the impression of an archipelago rather than a ridge crest.

3. Results

a. *RAFOS float trajectories over the Mid-Atlantic Ridge*

Figure 2 shows the trajectories of the 85 RAFOS floats launched west of the MAR during 1997–98 (open circles mark launch positions). The overall dominance of eastward flow between 45° and 53°N is evident, as is the high degree of eddy motion west and east of the MAR. Of particular interest to this study are the two streams of float trajectories emanating from the CGFZ and the FFZ on the eastern flank of the MAR, whose deep axes are defined here by the 3000-m isobath. These two clusters of floats remain distinct for about 100 km downstream, at which point they partially intermingle. The bulk of the floats then turned northeastward into the Iceland Basin, as discussed in more detail in Bower et al. (2002).

The apparent funneling of the floats over these two fracture zones is well illustrated by some individual float trajectories. Figure 3 shows the trajectories of four floats that crossed the ridge over the CGFZ, superimposed on high-resolution gridded bathymetry (Smith and Sandwell 1997) shaded in 500-m increments for water depth less than 3000 m. Table 1 gives the release dates and initial depths of these floats. They exhibit significant variability upstream and downstream of the ridge and approach the ridge at various latitudes, but they *cross* the ridge in a narrow latitude band over the

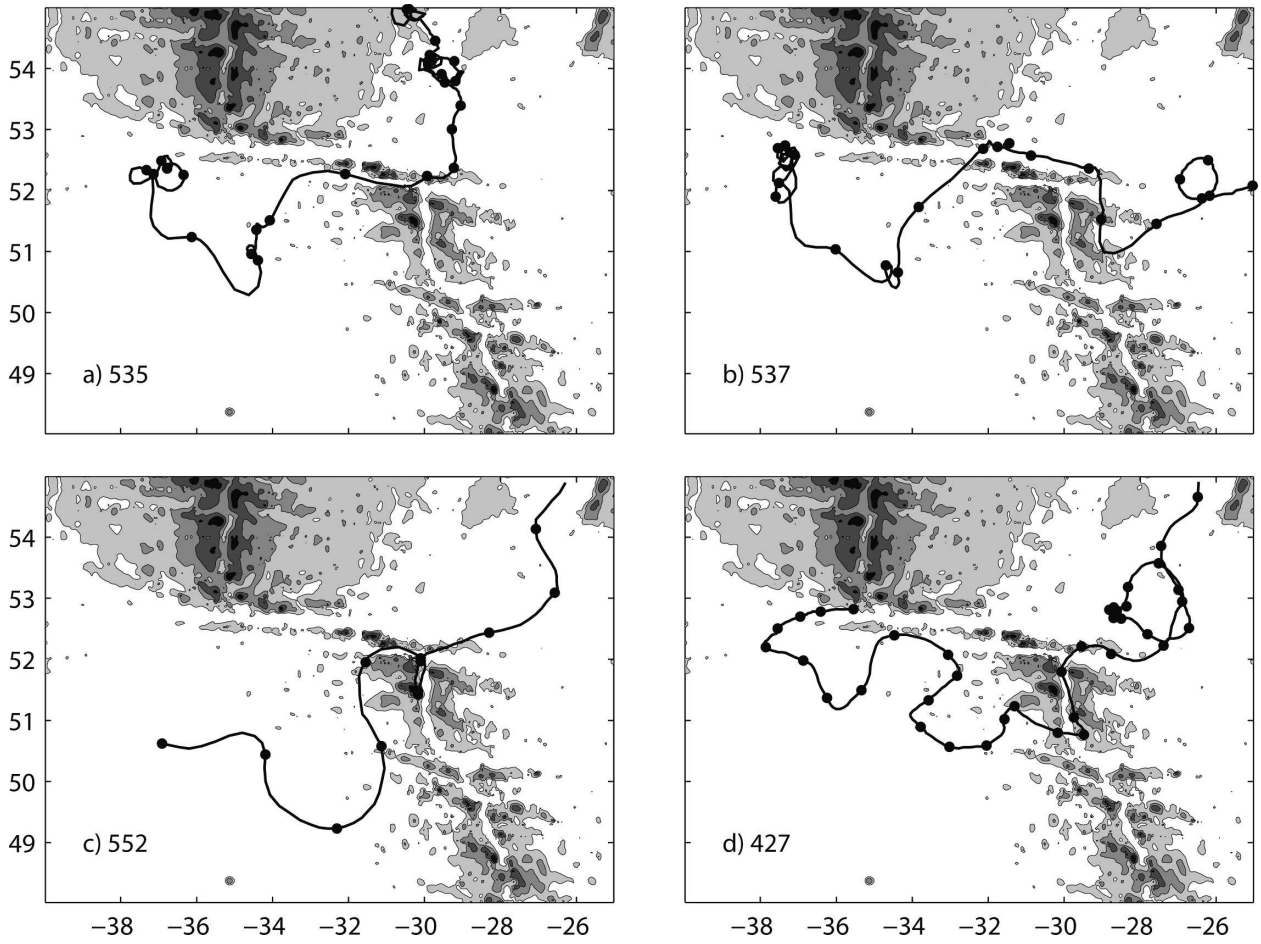

FIG. 3. Trajectories of four acoustically tracked RAFOS floats that crossed the MAR over the CGFZ (52°–53°N). Release dates and other characteristics of the floats are given in Table 1. Position is plotted daily, and large dots indicate position every 10 days. Bathymetry is shaded in 500-m intervals starting at 3000 m.

CGFZ. For the purposes of this study, a float is said to have crossed the ridge at the location where it passes over the central rift valley. In fracture zones, where there is no well-defined rift valley, the axis is defined as the line connecting the rift valleys north and south of the fracture zone. In cases where there are multiple crossings of the ridge axis (e.g., Fig. 3d), the last one is assigned as the float's crossing location.

Even though the floats were 1000–1500 m above the ridge crest, and therefore not physically constrained to cross over the ridge in any particular location, they crossed the ridge over deeper water, avoiding the higher terrain of the ridge crest. They were clearly influenced by small-scale features of the ridge. For example, float 427 (Fig. 3d), released just at the western end of the CGFZ in October 1997, initially drifted slowly westward for about 40 days before being entrained into the NAC (evident from increase in float speed and comparison with surface velocity, not shown). It meandered southeastward with the NAC, then crossed the western flank of the ridge in the FFZ in April 1998, turned sharply northward to follow the ridge's central rift valley in May 1998, and finally turned sharply eastward to cross the eastern flank of

TABLE 1. Float numbers, launch dates, and initial pressures after release and crossing pressures above MAR of eight floats shown in Figs. 3 and 4.

Float	Launch date	Initial pressure (dbar)	Crossing pressure (dbar)
535	23 Jul 1998	220.4	238.7
537	23 Jul 1998	95.9	192.3
552	24 Jul 1998	441.5	429.3
427	21 Oct 1997	458.5	565.2
422	21 Oct 1997	496.3	645.9
355	17 Oct 1997	701.0	659.4
534	24 Jul 1998	529.8	489.2
553	23 Jul 1998	188.4	531.0

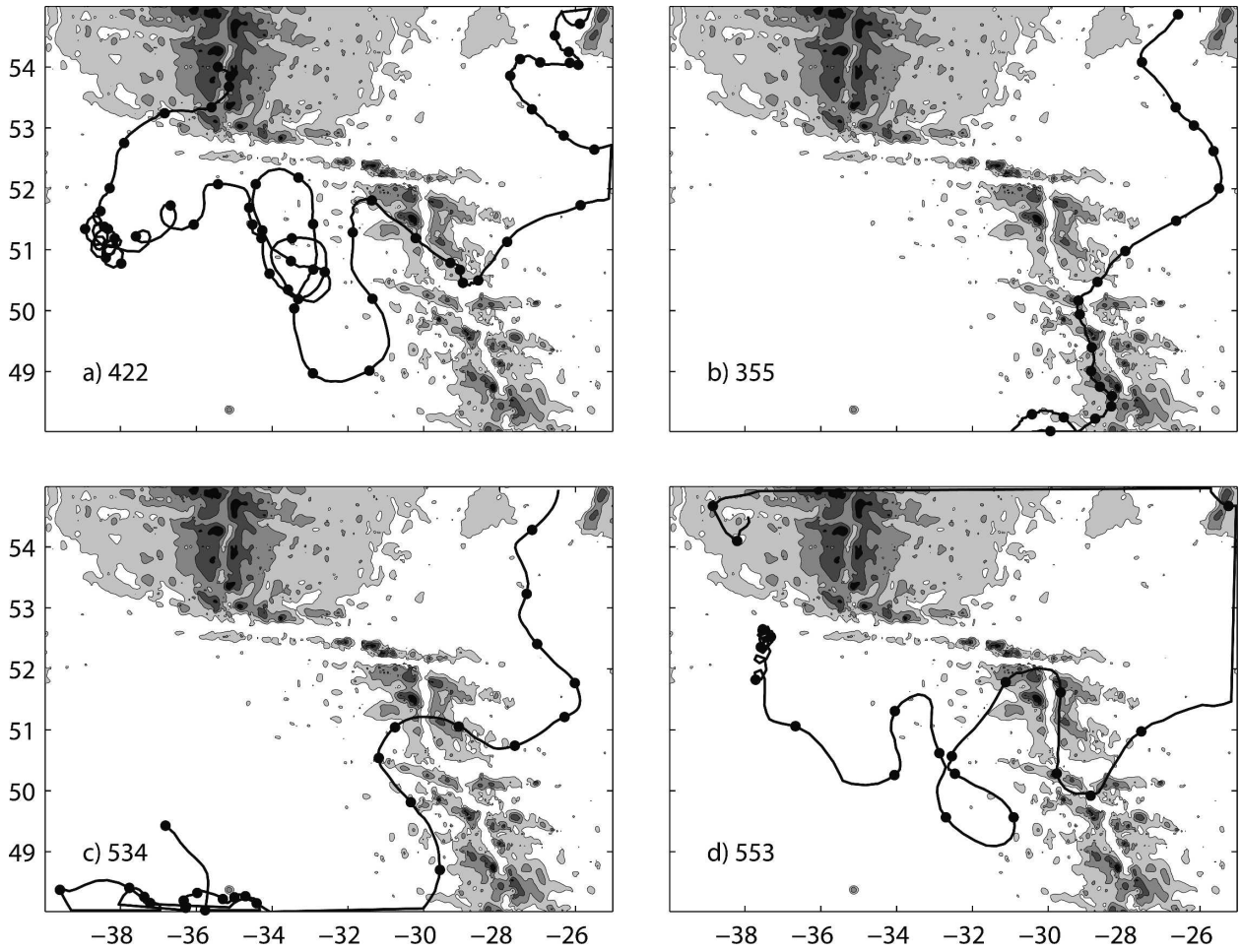

FIG. 4. As in Fig. 3 but for four floats that crossed the MAR over the FFZ (50°–51°N).

the ridge at the CGFZ. It was at a pressure of 565 dbar when it crossed the ridge, whereas the ridge crest is at about 2000–2500 m, with isolated peaks as shallow as 1000–1500 m.

Figure 4 similarly shows the trajectories of floats that crossed the ridge in the vicinity of the FFZ, the second widest and deepest gap in the MAR. These floats did not necessarily follow the FFZ as defined by the 3000-m contour, but they clearly avoided the shallower terrain of the ridge crest as they crossed the ridge in the vicinity of the FFZ. Float 553 (Fig. 4d) was, like 427 above, released near the western entrance to the CGFZ but in July 1998. About four months later, it crossed the western flank of the ridge in the southwestern part of the CGFZ, then turned sharply southward to follow the central rift valley in the opposite direction as 427 did half a year earlier. Float 553 finally crossed the eastern flank of the ridge through the FFZ. Note in this figure and the previous figure how some floats made long excursions along the western ridge flank before crossing over the fracture zones, consistent with earlier studies that showed large-amplitude meanders upstream of the ridge (Belkin and Levitus 1996). But the floats (and NAC branches) are much more latitudinally confined just where they flow over the ridge crest. This demonstrates the importance of tracing the current branches continuously over the ridge.

Bower et al. (2002) inspected all 85 float trajectories to determine the latitude of MAR crossing, and the results are presented in a histogram in Fig. 5, reproduced from Bower et al. (2002). Figure 5a shows how the RAFOS floats released west of the ridge were funneled over deep gaps in the ridge, especially the CGFZ and the FFZ. By comparing the distribution of launch latitudes (unshaded bars) to the distribution of crossing latitudes (red filled bars), it is evident that the floats were redistributed into narrower bands aligned with the fracture zones as they crossed the ridge. Using strict latitudinal limits for the definition of each gap, we find that two-thirds (42) of the 61 floats that crossed the

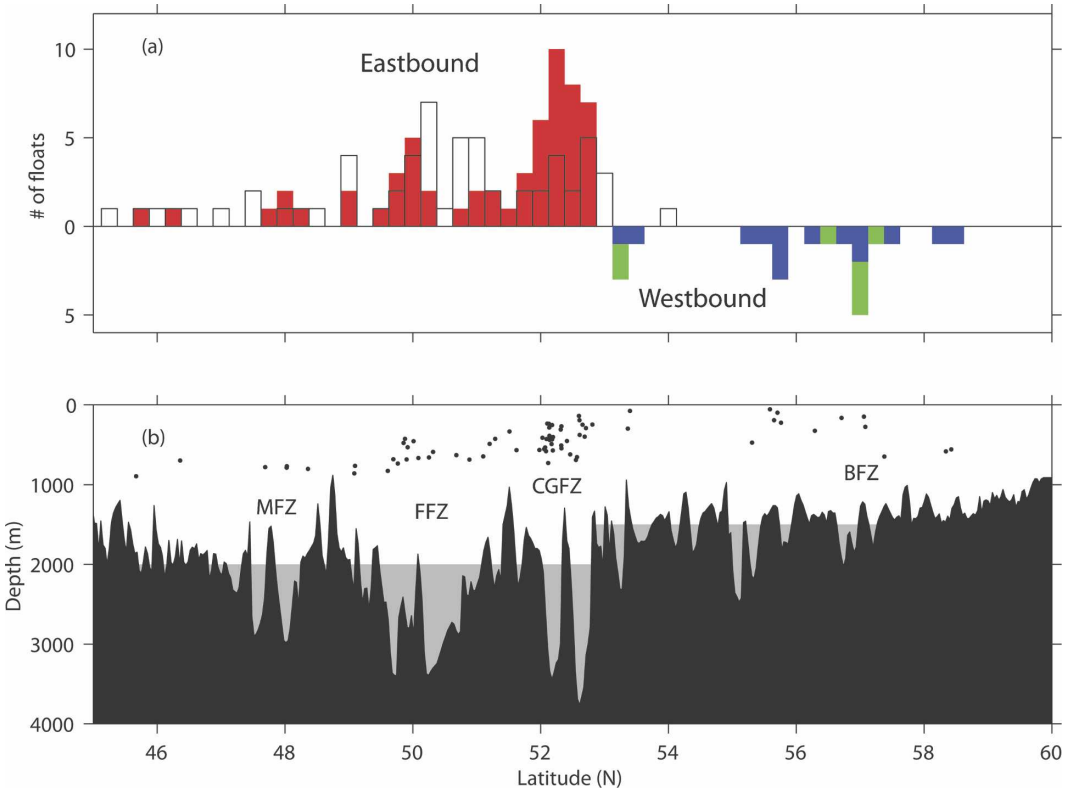

FIG. 5. (a) Distribution of latitudes where floats crossed the MAR. Crossing latitudes of floats are shown in filled bars. (b) Depth of ridge crest (defined as the minimum depth in a longitudinal band along the ridge crest, including both the eastern and western flanks) as a function of latitude, with float depth and latitude at time of ridge crossing (small dots). Major fracture zones are labeled. (Reproduced from Bower et al. 2002.)

ridge from west to east did so over the CGFZ and FFZ. A smaller group crossed over the MFZ. Figure 5b shows the depth of the ridge crest and the latitude and depth of each float where it crossed the ridge.

If we consider float crossings separated by 10 days [an estimate of the decorrelation time scale in the northwestern North Atlantic, Owens (1991)] or 100 km to be independent, there were approximately 50 independent crossing events over about 2.5 yr. In other words, even though all the floats were deployed on only 3 different cruises, variability in pathways resulted in about 50 independent realizations of floats crossing the ridge.

b. Comparison of float trajectories and satellite-derived geostrophic surface currents during 1998

The float trajectories shown above suggest that at least some of the branches of the NAC are constrained to cross the ridge not just over the CGFZ, as suggested in earlier studies, but also over the FFZ and MFZ. These float observations are fairly limited in time, however, so we chose to also analyze the longer time series of the MADT (1992–2006) and surface geostrophic velocities (hereinafter simply "velocities") derived from the MADT to further investigate the pathways of the NAC over the MAR and their variability. Our first step in this analysis was to determine if the flow patterns revealed by the subsurface RAFOS floats are qualitatively similar to those at the sea surface. In Fig. 6, we show the amplitude of the velocity vector (color shading) along with the velocity vectors for amplitude exceeding 0.1 m s^{-1} for three dates in 1998. The 3000-m isobath is superimposed as a heavy black line to outline the major features of the ridge bathymetry. Due to the somewhat coarse resolution of the MADT (⅓° × ⅓°), velocity amplitude is most likely underestimated in these plots, but the pathways of the main current branches (~100 km in width) should be well represented. Red shading indicates the highest speeds, and the continuous bands of red illustrate continuous branches of the NAC. Superimposed in white are 7-day float track segments, 3.5 days before and after the specified date of the image.

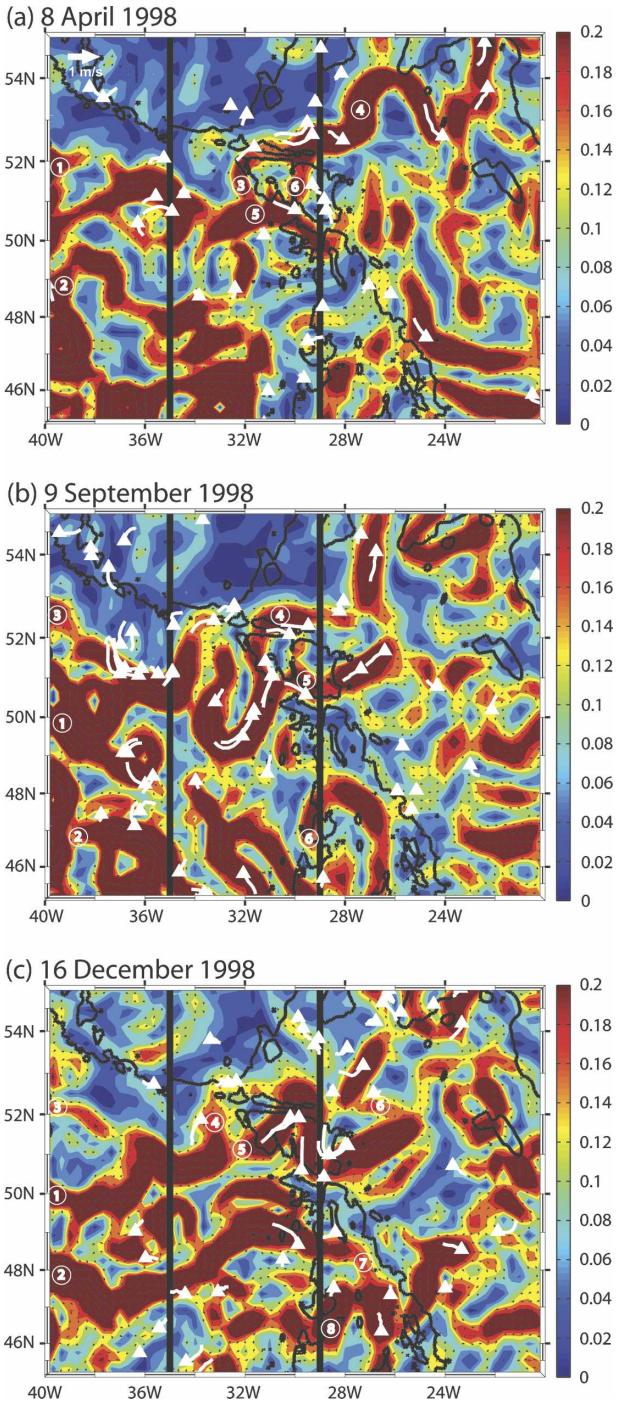

FIG. 6. Pathways of the NAC above the MAR on (a) 8 Apr, (b) 9 Sep, and (c) 16 Dec 1998. Contours and color shading show the amplitude of the surface velocity vector as derived from the MADT. Vectors indicate surface velocity greater than 0.1 m s^{-1}, with unit vector in the top-left corner. White lines show 7-day float track segments centered on the date of the image, with a triangle at the position of the last day indicating the heading. The 3000-m isobath is shown in black and 35° and 29°W transects of Fig. 7 are indicated by black lines.

The first and most important point to take away from these images is that the float track segments are generally well aligned with the surface currents, and float velocity is qualitatively positively correlated with surface velocity. This is an important finding, as it directly compares the well-established Lagrangian float data with the relatively new data acquisition and processing techniques used for the satellite altimetry and gives credibility to the latter. We highlight particularly striking features in each of the three images as follows.

- 8 April 1998 (Fig. 6a): We focus first on the two strong NAC branches flowing quasi-eastward across the western part of the study region, the northern branch (segment 1) originating at about 52°N flowing first southward along 40°W to 50.5°N before turning eastward, and the southern branch (segment 2) flowing northward past 49°N before turning eastward. The northern branch meanders right up to the western flank of the MAR at about 50.5°N, where it splits into two parts. The northern part (segment 3) flows northward along the western flank of the ridge to the latitude of the southern transform valley of the CGFZ[1] where it turns sharply eastward to flow over the fracture zone. Several RAFOS floats are drifting over the gap at the same time, indicating that this branch reaches down to at least the main thermocline. After exiting the CGFZ, this branch meanders northeastward, with several RAFOS floats embedded, toward the Rockall Plateau (segment 4). The southern part of the northern branch (segment 5) continues eastward through the FFZ, but at the ridge crest, a part (segment 6) turns sharply northward to follow the ridge's central rift valley and joins the branch in the CGFZ (segments 3–4). The remainder continues through the FFZ, and then seems to break up into a number of discrete eddies in the eastern basin. The southern branch (segment 2) meanders eastward then southeastward and out of the study area before crossing the ridge. Three floats lined up along the western flank of the ridge (29°W) between 46° and 49°N also show no indication of an eastward current branch flowing over the ridge in this latitude band.
- 9 September 1998 (Fig. 6b): The number of RAFOS floats in the study area reached a maximum during this time period. Again, two strong branches of the NAC are meandering across the western part of the study region, one entering at about 50°N (segment 1)

[1] The CGFZ has two east–west transform valleys, separated by a median ridge (Fig. 1b). The sills for the northern and southern valleys are at about 35° and 30°W, respectively (Seale 1981).

and the other at about 47°N (segment 2). A weaker third branch enters at about 53°N (segment 3), but it merges with (segment 1) before reaching 35°W. After crossing 35°W, the merged branches (segments 1 and 3) form a large-amplitude backward S-shaped meander, which is also revealed by a number of the floats. This meander ends with the branch flowing northward along the western flank of the ridge. It then splits into two subbranches, one that continues northward to the CGFZ (segment 4) and the other which turns east over the FFZ (segment 5). The CGFZ branch (segment 4) meanders northeastward as a strong continuous current branch, while the FFZ branch (segment 5) continues eastward and seems to weaken and break up somewhat into eddies in the eastern basin. These two branches remain more or less distinct in the eastern basin. The original southern branch (segment 2) meanders strongly as it flows eastward. At about 29°W, it is flowing northward along the western flank of the MAR (segment 6). It crosses the ridge crest near the latitude of the MFZ (see Fig. 1b) and then turns sharply southward to follow the eastern flank of the ridge crest and leaves the study region to the south.

- 16 December 1998 (Fig. 6c): At this time, there are again two strong branches entering the region from the west, at 50°N (segment 1) and 48°N (segment 2). A thinner branch is also apparent entering at 52°N (segment 3) but, as in Fig. 6b, this branch merges with (segment 1) before reaching 35°W. After crossing 35°W, this merged branch splits: the weaker part (segment 4) turns northward to the CGFZ while the stronger part (segment 5) cuts over the western ridge crest, then turns sharply southward to follow the rift valley, and turns sharply again to the east to exit the ridge area over the FFZ. Several floats also reveal this pathway, including 553, which is drifting due south over the rift valley (see also Fig. 4d). After leaving the FFZ, this branch meanders back northeastward (segment 6), but maximum surface speeds are lower and the current branch appears less continuous compared to the two previous images. The original southern branch (segment 2) heads eastward and crosses the ridge near the MFZ as before (segment 7), then turns southward and merges with a stronger branch that crossed the ridge farther south (segment 8). The merged result meanders northeastward and does not appear to interact with the northern branches in the study area.

On all three dates shown, the pathways of the NAC branches at the surface are qualitatively confirmed by the float movements. The greater spatial coverage of the satellite-derived surface velocities shows that 1) two current branches enter the region from the west on all three occasions, one between 50° and 52°N and the other between 46° and 48°N; 2) the northern branch is apparently steered significantly by the topography of the ridge, either splitting into two branches, one passing over the CGFZ and the other over the FFZ, or passing from one gap to the other via the ridge's central rift valley; and 3) the southern branch is more variable in its extension over the ridge, but passes in the vicinity of the MFZ on two of the three occasions shown here. In the next section, we will show that the splitting pattern over the CGFZ and FFZ persisted for several years in the late 1990s.

c. Temporal variability in NAC branches from 1993 to 2006

In this section, we use surface geostrophic velocity derived from the MADT to examine the temporal variability in the location of the NAC branches near the MAR from 1993 to 2006. To focus attention on the interannual time scale, the zonal and meridional components of velocity at each grid point were low-pass filtered using a third-order Butterworth filter with a cutoff period of 90 days. Then the zonal velocity component along 35° and 29°W was plotted against time (Fig. 7). Small charts to the right show the bathymetry shallower than 3000 (light shading) and 2500 m (dark shading) for a 250-km-wide longitudinal strip along each transect. From these charts, it is apparent that the 35°W transect is upstream of the MAR crest south of 53°N (upper chart). The 29°W transect is located just downstream of the MAR crest at the latitude of the CGFZ, at the ridge crest at the latitude of the FFZ, and west of the MAR crest south of about 49°N (lower chart; see also Fig. 1b).

The color panels in Fig. 7 show eastward velocity ranging up to 0.3 m s^{-1} (red) and westward velocity as high as -0.3 m s^{-1} (blue). To identify the prevalent pathways of the NAC, continuous (in time) strong eastward velocity features were connected by eye. This subjective method draws upon some assumptions. It was assumed that the NAC is indicated by strong eastward flow across the transects. This flow would peak at one or more latitudes for a particular time, representing one or more branches of the NAC. Due to the relatively slow evolution of the velocity field, the branches would not jump discontinuously between latitudes, but changes would be gradual and continuous. Peaks of eastward velocity were connected by transparent black lines, if they would connect to neighboring features for at least a period of one year. The line thickness was

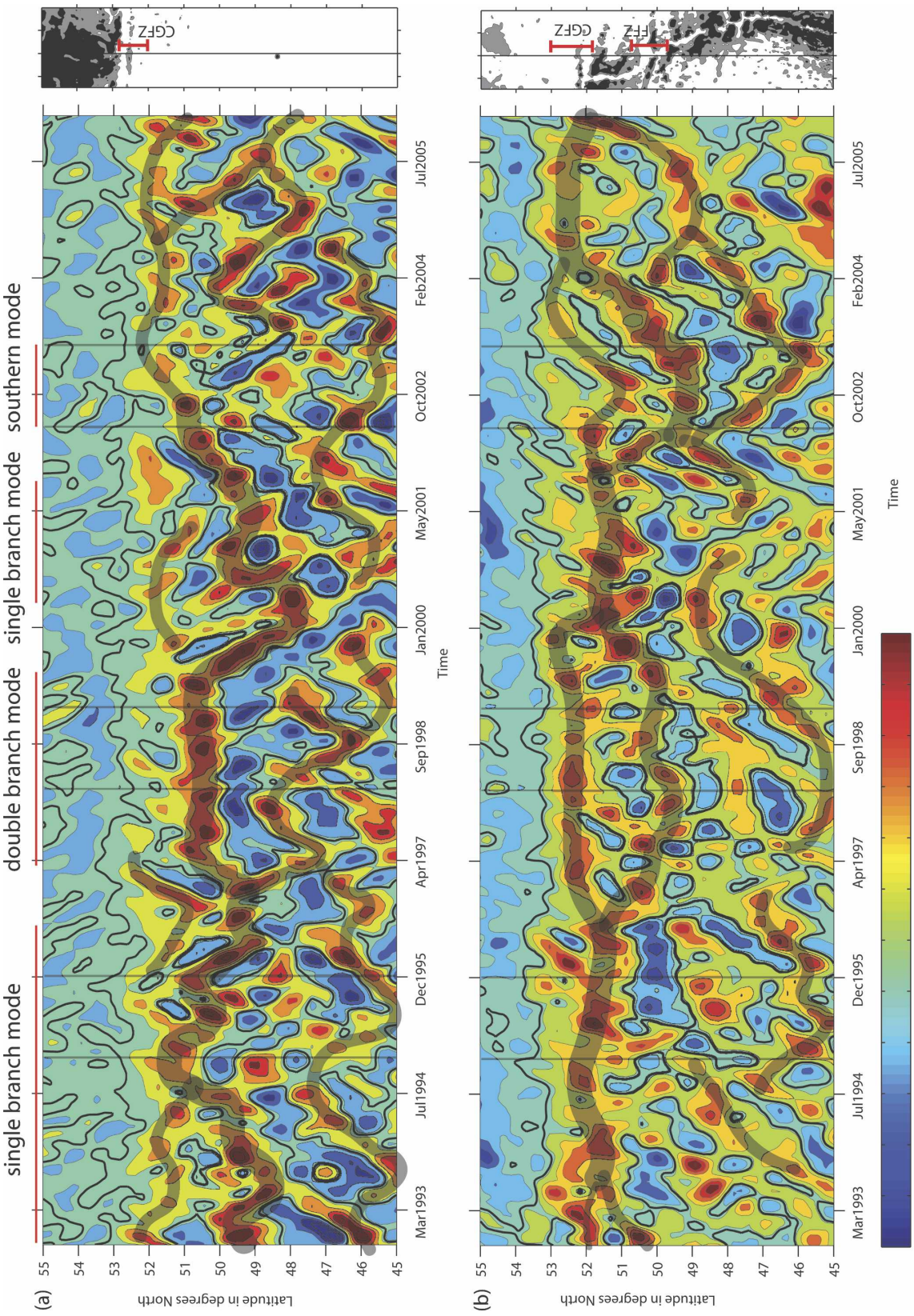

FIG. 7. Latitude vs time plots of zonal velocity (a) at 35° and (b) at 29°W. Contours show 90-day low-pass filtered MADT derived surface geostrophic eastward velocity with the heavier black line indicating zero speed. Branches are defined in the top line and also pointed out by transparent black lines. Vertical lines indicate time periods for Fig. 8. Small charts at the right show bottom depth shallower than 3000 (light shading) and 2500 m (dark shading) in a 250-km-wide strip along each transect, which is marked with vertical lines.

chosen to be bigger either for stronger velocities or for wider currents.

At the upstream transect (35°W, Fig. 7a) the most northern continuous contour of zero zonal velocity (thick black contour), marking the northern edge of the NAC system, ranges between 52° and 54°N with the mean around 53°N, the latitude of the northern edge of the CGFZ. For the period up to the end of 2002 there is one dominant eastward current branch that is observed at various latitudes between 48° and 52°N. This is the northern branch of the NAC (SPF). During this same time period a second but weaker branch was observed most of the time, mainly between 45° and 47°N. This appears to be what Belkin and Levitus (1996) referred to as the Mid-Atlantic Front, originating from the northward flowing NAC east or southeast of Flemish Cap. These two main branches west of the MAR are clearly evident in Fig. 6. A third branch was observed between 51°and 52°N only when the dominant branch was in a southerly position. This may be related to the splitting of the SPF downstream of the Northwest Corner noted by Belkin and Levitus (1996), but it appears not to be a persistent feature. Note from the chart on the right that the current branches crossing this transect are relatively unconstrained by bathymetry. Only the northern branch appears to be limited in its northward excursions (dynamically, not physically) by the Reykjanes Ridge at about 53°N. This would be consistent with the large latitudinal shifts observed in the NAC branches for much of the record.

From April 1997 until September 1999 the dominant northern branch is unusually stationary at 50.5°N. From September 1999 until February 2000 it traverses steadily southward, reaching a minimum latitude below 48°N in early 2000. From October 2002 on, there is no dominant branch crossing 35°W, but rather several weaker branches, the northern of which is the steadiest at a latitude of about 52°N.

At 29°W (Fig. 7b) the northern contour of zero zonal velocity is found somewhat farther north than at 35°W, ranging between 53° and 54°N with the mean around 53.5°N. For the time period up to September 1996 there is a dominant broad NAC branch mainly located between 51° and 52.5°N, the latitudes of the southern part of the CGFZ at this longitude (see chart at right). This branch is much more stable than the dominant branch at 35°W for the same time period (Fig. 7a), reflecting the constraint imposed by the bathymetry of the ridge. During this time there are some multimonth periods of strong westward flow centered at 50°N, and some relatively weak discontinuous eastward-flowing branches to the south.

In September 1996, the dominant branch crossing 29°W splits into two branches that are individually weaker than the original, but similarly stable in latitude. The northern branch consistently stays at 52.5°N, the central latitude of the CGFZ, whereas the southern branch meanders between 49.5° and 50.5°N, a latitude band that includes the FFZ. It was approximately during this same time period that the dominant branch at 35°W was apparently locked to 50.5°N. The double branching of the SPF at 29°W was observed by many of the RAFOS floats (see section 3a): synoptic views can be seen in Fig. 6. In July 1999 the two branches start to rapidly reconnect and form one strong single branch in January 2000. Note that the reconnection is preceded by one or two months by an "unlocking" of the dominant branch at 35°W and its southward migration. In January 2002 a rapid southward transition of the dominant branch crossing 29°W takes place and just for one year between April 2002 and April 2003 this branch is between 49° and 49.5°N, the latitude of the >2500 m deep gap just south of the FFZ. Throughout the following year the branch migrates back northward and from April 2004 till the end of the record there is stationary flow at the latitude of the CGFZ both at 29° and at 35°W. From April 1997 onward, there is almost always a weak branch crossing 29°W between 45° and 48°N. This contrasts with the earlier part of the record where there was little evidence of a persistent southern branch crossing the transect.

Figure 7b shows that there are at least three clearly identifiable "modes" by which the northern branch of the NAC crosses the MAR. From 1993 to 1996 and from 2000 to 2002 we see a single dominant branch on both sides of the ridge (single branch mode). Upstream the single branch meanders significantly between 48° and 52°N, while downstream of the ridge, it is on average farther north and more stable at about 52°N, indicating the dynamical constraint of the CGFZ. The two-dimensional structure of this and the other branching modes will be discussed in section 3d. From 1997 to 1999 (i.e., the float time period), we see a single branch upstream and a double branch downstream of the MAR (double branch mode). For most of this time period, the upstream branch is strongly constrained in latitudinal extent, apparently locked at 50.5°N. The two branches downstream are aligned with the CGFZ and FFZ. In 2002–03 the dominant branch upstream weakens and the dominant branch downstream shifts rapidly southward by several degrees and remains there for the year (southern mode). In addition to this there are several transitory situations (e.g., 2001/02). There are no similar modes apparent for the southern NAC branch: it shows no "preferred" latitudes. This may be due to

the fact that both transects are west of the ridge crest south of about 49°N (Fig. 1b).

d. Spatial structure of the three branching modes

To document the spatial structure of the three branching modes, the MADT-derived zonal and meridional velocities were averaged over one year that is representative of the respective modes to obtain the mean velocity vectors for each grid point for each time period. Figure 8 contours the amplitude of the mean velocity vectors, with maxima of 0.2 m s^{-1} in red, and the mean velocity vectors for each AVISO grid point for amplitudes larger than 0.1 m s^{-1}. As in Fig. 6, the 3000-m isobath is superimposed for reference. The time periods of the modes according to Fig. 7 were chosen to be 1 January 1995–1 January 1996 for the single branch mode (Fig. 8a), 1 January 1998–1 January 1999 for the double branch mode (Fig. 8b), and 1 April 2002–1 April 2003 for the southern mode (Fig. 8c). Other averaging periods chosen from the respective modes showed nearly identical structures.

The single branch mode in Fig. 8a is characterized by strong eastward mean flow across 35°W at about 51°N. That flow splits up and the northern part goes over the southern as well as the northern transform valleys of the CGFZ. It flows straight east over the CGFZ and leaves it with a southeastward curvature with the velocity maxima following the bathymetry. Because this branch was deflected northward to pass through the CGFZ, it crosses 29°W farther north than it did 35°W, at 52°N. There is low amplitude mean westward flow into the FFZ. Weaker eastward flow across the MAR also occurs between 48.5° and 49.5°N as well as between 45° and 46.5°N.

The double branch mode in Fig. 8b is characterized by a strong southeastward mean flow across 35°W between 50° and 51°N (same latitude but different direction, cf. 1995). It curves northward around 32°W, and part of the flow enters the western end of the FFZ, becomes weaker in the FFZ, and exits the FFZ northeastward in a strong stationary flow. The other part of the flow passes across the western edge of the MAR to leave the southern part of the northern CGFZ transform valley straight eastward before turning northward around 53°N, 27°W. Although the branches appear somewhat weaker and more discontinuous in this annual mean view compared to the synoptic views in Fig. 6, they still appear as distinct branches east of the MAR. As the meridional flow through the rift valley shown in Fig. 6 changes direction throughout 1998, it gets averaged out in Fig. 8b. Weaker eastward flow across the MAR also occurs between 47° and 48.5°N in a current branch that flows up from the south along the

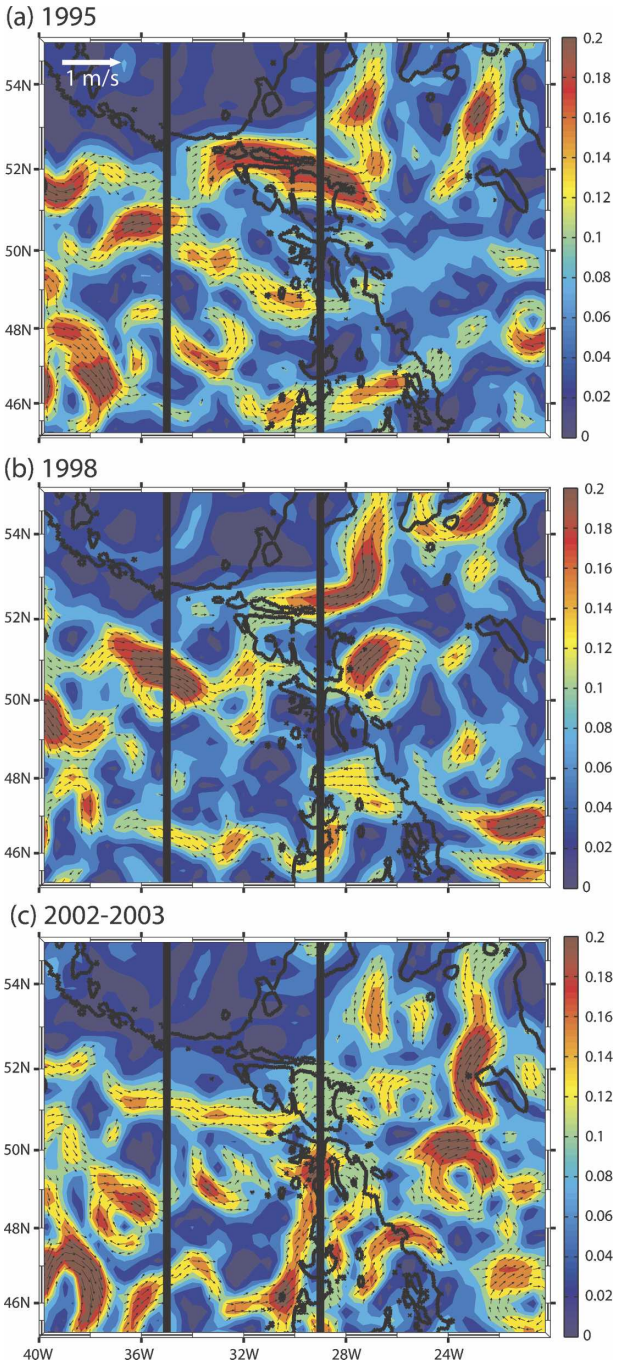

FIG. 8. Annual average pathways of the NAC above the MAR in (a) January 1995–December 1995, (b) January 1998–December 1998, and (c) April 2002–March 2003. Contours show amplitude of the mean surface velocity vector for the respective year as derived from the MADT. Vectors indicate mean geostrophic surface velocity greater than 0.1 m s^{-1} with unit vector in the top-left corner. The 3000-m isobath is shown in black and 35° and 29°W transects of Fig. 6 are indicated by the black lines.

western flank of the ridge until the latitude of the first gap deeper than 2500 m (see chart in Fig. 7b).

The southern mode (2002–03, Fig. 8c) is strikingly different from the previous two modes. It is first characterized by generally weaker annual mean flow in the current branches upstream of the ridge. Three current branches cross 35°W, but there is no dominant branch. A weak northern branch enters the FFZ, but then turns northward and spreads out over the shallow eastern ridge crest. The strongest mean flow crossing 29°W is south of the FFZ between 49° and 50°N, several degrees south of the dominant current branches for the other time periods. It comes up from 46°N, 32°W and flows straight north along the 3000-m isobath. It turns east and then south around 50°N, 28°W, and part of it flows back south along the 2500-m isobath before it turns around again at 46°N to flow northeastward over the MAR. The entire CGFZ has flow close to zero, also completely unlike the other modes.

4. Discussion and summary

Earlier studies have suggested that the northern branch of the NAC is somewhat constrained to cross the MAR over the CGFZ (Sy 1988; Sy et al. 1992; Belkin and Levitus 1996). This description was constructed mainly based on hydrographic sections collected upstream and downstream of the ridge crest. Here we have for the first time attempted to trace the pathways of the NAC branches continuously across the MAR in relation to high-resolution bathymetry and to document temporal variability in those pathways using subsurface float observations (1997–99) and satellite-derived geostrophic surface velocity observations (1992–2006). We have shown that, while this pattern can persist for years at a time, other persistent patterns are possible, including a double branching mode and a southern mode. In the double branching mode, observed from 1996 to 1999, the northern NAC branch split into two, one passing over the CGFZ and the other over the FFZ. The resulting two branches often remained distinct for at least several hundred kilometers downstream of the MAR, indicating that the shallow part of the MAR between the CGFZ and FFZ can permanently split one current branch into two. In the southern mode, observed in 2002–03, the dominant NAC branch (which was considerably weaker than in other years) crossed the MAR several degrees south of the CGFZ, through a gap deeper than 2500 m near 49°N. At this time there was almost no eastward surface flow at the latitude of the CGFZ.

The cause for these interannual changes in the pathways of the NAC where they cross the MAR is at this point unknown and remains to be studied. White and Heywood (1995) found some correlation between the number and location of NAC branches and interannual changes in the location of the zero contour of winter wind stress curl using *Geosat* (1986–88) and the first two years of TOPEX/Poseidon data (1992–94), although interannual latitudinal shifts in the wind stress pattern were found to be much larger than shifts in the NAC branches. Previous studies have linked variability in subpolar gyre circulation and pathways to the phase of the NAO (e.g., Bersch et al. 1999; Curry and McCartney 2001; Flatau et al. 2003; Häkkinen and Rhines 2004). Bersch et al. (1999) showed that the eastern limb of the subpolar gyre contracted westward after a large drop in the NAO index in the winter of 1995/96.

In Fig. 9, we show the last 26 years of the average NAO index, as computed by the National Centers for Environmental Prediction (NCEP) based on an analysis of teleconnection patterns. At the beginning of our study period (1993), the NAO index was in the middle of a strong positive phase that had begun in the late 1980s. In the winter of 1995/96, the index fell precipitously to very low values. At about the same time, the dominant NAC branch at 35°N started migrating southward and, later in 1996, it split into two branches, one over the CGFZ and one over the FFZ. In the next few years, the NAO index fluctuated somewhat but remained negative, and the NAC double branching mode persisted. In 1999, the index returned to high positive values, and the NAC returned to a single branch mode. During 2001–04, the NAO index was again decreased to neutral values or slightly negative and it is during this time period that the southern branch mode was observed (2002–03). The correspondence between the changes in the NAC pathways and the NAO index is remarkable. However, we cannot talk about a causal relationship here as, for example, Eden and Willebrand (2001) have shown in the context of a high-resolution numerical model of the North Atlantic that the response of the subpolar gyre to changing wind and buoyancy forcing is complex and includes both short time-scale barotropic and long time-scale baroclinic components. More study is needed here, especially comparing the annual wind stress curl patterns to the annual mean flow patterns, as was done for a few years for the whole subpolar gyre by White and Heywood (1995).

The pathways of the NAC over the MAR may have significant implications for the deep, as well as shallow, limb of the meridional overturning circulation (MOC). An absolute velocity section across the CGFZ at 35°W in August 1997, reported by Schott et al. (1999), indicated top-to-bottom eastward flow associated with a

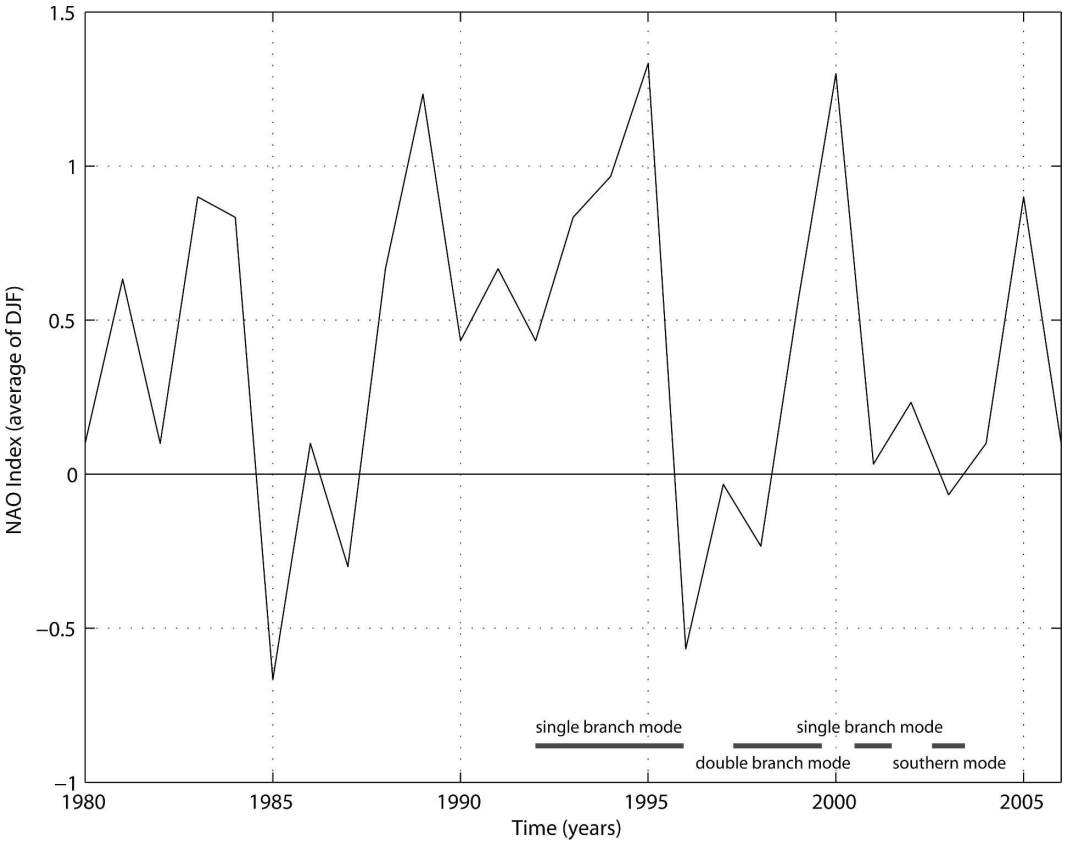

FIG. 9. North Atlantic Oscillation (NAO) index averaged for the winter months (December–February) from 1980 to 2006 estimated from monthly mean values provided by NCEP based on an analysis of teleconnection patterns.

northward excursion of the NAC, with surface velocities of about 0.2 m s^{-1}. The westward flow often observed in the northern channel of the CGFZ at depth that is associated with passage of Iceland–Scotland Overflow Water (ISOW) from the eastern North Atlantic into the western basin (e.g., Dickson and Brown 1994; Saunders 1994) was completely absent in this synoptic velocity section. Schott et al. (1999) noted a number of other isolated observations of northward excursions of the NAC's northern branch and speculated that the portion of the deep MOC originating in the eastern basin may be temporarily blocked or seek other routes across the MAR when the NAC is in such a northern position.

To place the Schott et al. (1999) results in the context of the present study, Fig. 10 shows the amplitude of the monthly mean velocity for the time of the Schott et al. measurements, August 1997, with contemporaneous RAFOS float track segments superimposed (as in Fig. 6). We see an eastward surface flow at 35°W centered at about 52.3°N, coincident with the deep-reaching NAC branch observed by Schott et al. (white line at 35°W). Figure 10 shows that this current was a branch from a stronger NAC branch that crossed 35°W at about 51°N, south of the Schott et al. section.

From the time series in Fig. 7a, we can determine the temporal distribution of eastward velocity at the location investigated by Schott et al. (1999). A time series of zonal velocity at 52.3°N, 35°W, in Fig. 11a (produced from same data as Fig. 7a) shows that most of the time eastward (positive) flow was observed at the surface at this site. However, an eastward surface current does not necessarily mean that the deep westward flow is blocked. Since we have no simultaneous measurements of the deep flow for the satellite time series, we turn to the synoptic section of Schott et al. for guidance, recognizing that it may or may not be representative. Along with a maximum eastward surface velocity of 0.2 m s^{-1}, they observed an average eastward deep flow of about 0.05 m s^{-1}. If we assume that this vertical shear remains more or less constant, then a minimum eastward speed of 0.15 m s^{-1} at the surface would be required to block the westward flow at depth. From Fig. 11b, we see that an eastward flow of at least this magnitude occurred only 6% of the time between 1993 and 2006, that is, relatively rarely. This should probably be

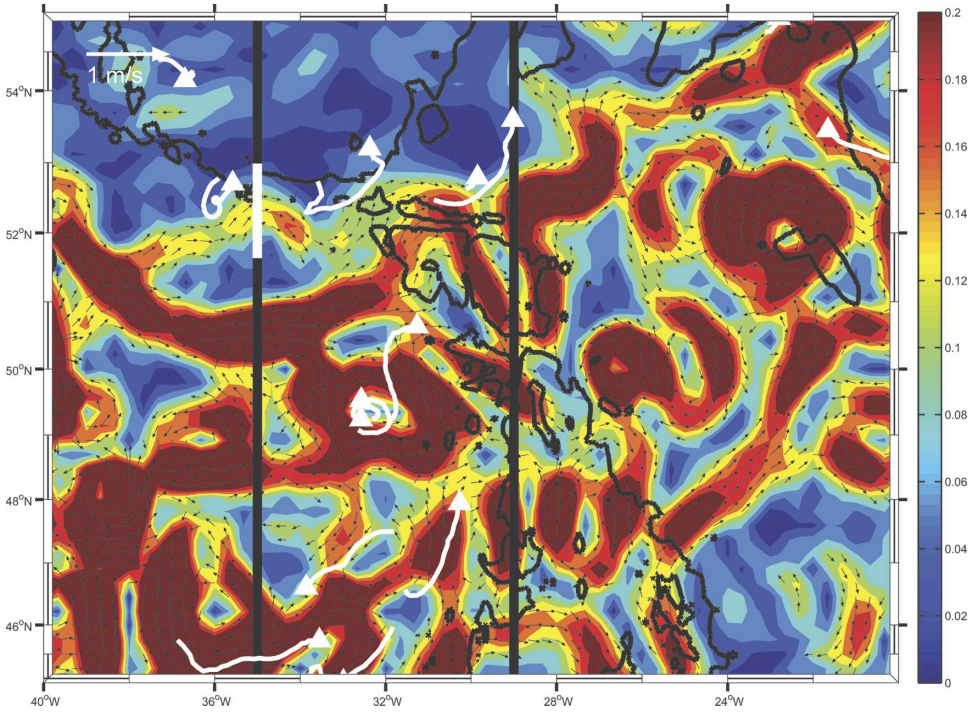

FIG. 10. As in Fig. 6 but for monthly mean pathways of the NAC above the MAR in August 1997, which was the month of R/V *Meteor* cruise of Schott et al. (1999). The white bar indicates the *Meteor* transect from 51.6° to 53.0°N along 35°W.

considered a lower bound since the gridded surface geostrophic velocities derived from altimetry are somewhat underestimated. There is considerable interannual variability in strong eastward currents. For example, no eastward flow greater than 0.15 m s^{-1} was observed in the satellite data between June 1998 and June 2000 (no blocking), while it occurred 35% of the time during the 12-month period June 2001–June 2002 (considerable blocking). The average length of the six events with low-passed eastward velocity in excess of 0.15 cm s^{-1} that occurred over the entire time series is about 50 days (Fig. 11a).

From a 1-yr deployment of deep (depth $\geq$ 2500 m) current meters across the CGFZ at 35°W, Saunders (1994) found that the deep transport was eastward (like reported by Schott et al. 1999) about 15% of the time (see his Fig. 10), which falls within our observed range of 0%–35% for a given 12-month period. Unfortunately, the current meter moorings did not extend above 2500 m, so correlations of eastward flow at depth with eastward flow at the surface cannot be determined.

In conclusion, we have shown that during 1992–2006, there is a strong correlation between the latitude where the northern branch of the NAC (SPF) crosses the MAR and the location of deeper gaps in the ridge. This current branch was found most often over the CGFZ, but for one or more years all or part of it was also found over other gaps in the MAR. During 1997–99, the northern NAC branch clearly split into two branches where it impacted the ridge, with one branch passing over the CGFZ and the other over the FFZ. Remarkably, these branches remained distinct for hundreds of kilometers downstream of the ridge, demonstrating how the bathymetry of the ridge can have a significant impact on the circulation downstream, including surface currents. In 2002–03, the dominant NAC branch was weaker and crossed the ridge several degrees south of the CGFZ. Some correspondence between the changes in branching modes and the NAO index was observed, but more analysis of the combined surface velocity and wind stress patterns is needed to draw firm conclusions. The weaker southern NAC branches were observed to be more variable in latitude, possibly because the two sections analyzed here were located upstream of the shallowest bathymetry associated with the ridge crest in the southern part of the study region. Some synoptic images showed a southern branch crossing 29°W between 45° and 47°N, then turning sharply northward to follow the western flank of the ridge before crossing the ridge over the first gap in the 2500-m isobath near 47.5°N. We suspect that a more detailed analysis of the southern NAC branches would find that

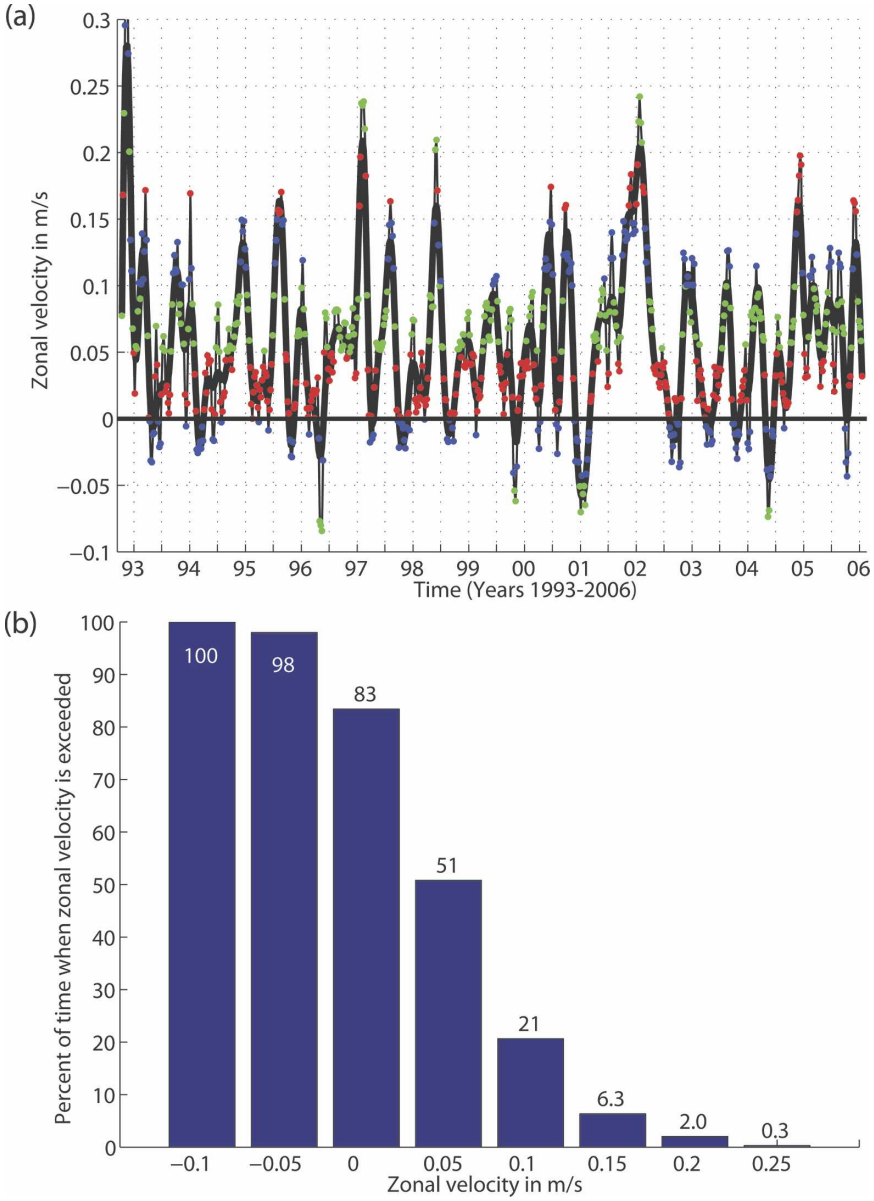

FIG. 11. (a) Time series of zonal velocity at 52.3°N, 35°W for the time period of the satellite observations, taken from Fig. 7. Data points (circles) are color coded by velocity range. A thin black line connects data points and the thick black line is zonal velocity low passed at 90 days. (b) Cumulative histogram of zonal velocity at 52.3°N, 35°W from Fig. 7. Numbers indicate the percent of observations that are at or above the value on the *x* axis.

they generally cross the ridge over the several deeper passes between 47° and the FFZ at 50°N, including the MFZ.

The deeper gaps in the ridge, especially the CGFZ, represent significant "choke points" in the MOC, where the deep and shallow limbs of the MOC are brought together, similar to the Gulf Stream–deep western boundary current crossover at Cape Hatteras (35°N, 75°W). We have discussed the possible blocking of the flow of ISOW through the CGFZ by northward excursions of the NAC, but perhaps, conversely, variability in the transport of overflow water has some impact on the pathways of the NAC. Simultaneous measurements of the deep and shallow velocity field over the MAR, which at present are almost nonexistent, are needed to gain a better understanding of the interactions between these major components of the MOC as they pass over the MAR.

Acknowledgments. The authors gratefully acknowledge Phil Richardson for early work on the float trajectories over the MAR and Heather Furey for assistance in the final preparation of this manuscript. Thoughtful comments from two reviewers helped to clarify several points in the manuscript. This research was supported by National Science Foundation Grants OCE-9531877 to the Woods Hole Oceanographic Institution (WHOI) and OCE-9906775 to the University of Rhode Island, by the WHOI Summer Student Fellowship Program, and by the Lawrence J. Pratt and Melinda M. Hall Endowed Fund for Interdisciplinary Research at the Woods Hole Oceanographic Institution.

REFERENCES

Anderson-Fontana, S., P. Lazarevich, P. Perez-Brunius, M. Prater, H. T. Rossby, and H.-M. Shang, 2001: RAFOS float data report of the Atlantic Climate Change Experiment (ACCE) 1997–2000. Graduate School of Oceanography, University of Rhode Island Tech. Rep. 01-4, 112 pp.

Belkin, I. M., and S. Levitus, 1996: Temporal variability of the Subarctic Front near the Charlie-Gibbs Fracture Zone. *J. Geophys. Res.,* **101,** 28 317–28 324.

Bersch, M., J. Meinke, and A. Sy, 1999: Interannual thermohaline changes in the northern North Atlantic 1991–1996. *Deep-Sea Res.,* **46,** 55–75.

Bower, A. S., and Coauthors, 2002: Directly measured mid-depth circulation in the northeastern North Atlantic Ocean. *Nature,* **419,** 603–607.

Curry, R. G., and M. S. McCartney, 2001: Ocean gyre circulation changes associated with the North Atlantic Oscillation. *J. Phys. Oceanogr.,* **31,** 3374–3400.

Dickson, R. R., and J. Brown, 1994: The production of North Atlantic deep water: Sources, rates, and pathways. *J. Geophys. Res.,* **99,** 12 319–12 342.

Eden, C., and J. Willebrand, 2001: Mechanism of interannual to decadal variability of the North Atlantic circulation. *J. Climate,* **14,** 2266–2280.

Flatau, M. K., L. D. Talley, and P. P. Niiler, 2003: The North Atlantic Oscillation, surface current velocities, and SST changes in the subpolar North Atlantic. *J. Climate,* **16,** 2355–2369.

Furey, H., A. Bower, and P. Richardson, 2001: Warm water pathways and intergyre exchange in the northeastern North Atlantic: ACCE RAFOS float data report. Woods Hole Oceanographic Institution Tech. Rep. WHOI-01-17, 153 pp.

Häkkinen, S., and P. B. Rhines, 2004: Decline of Subpolar North Atlantic circulation during the 1990s. *Science,* **304,** 555–559.

Heywood, K. J., E. L. McDonagh, and M. A. White, 1994: Eddy kinetic energy of the North Atlantic subpolar gyre from satellite altimetry. *J. Geophys. Res.,* **99,** 22 525–22 539.

Krauss, W., 1986: The North Atlantic Current. *J. Geophys. Res.,* **91** (C4), 5061–5074.

Owens, W. B., 1991: A statistical description of the mean circulation and eddy variability in the northwestern Atlantic using SOFAR floats. *Prog. Oceanogr.,* **28,** 257–303.

Rio, M.-H., and F. Hernandez, 2004: A mean dynamic topography computed over the world ocean from altimetry, in situ measurements, and a geoid model. *J. Geophys. Res.,* **109,** C12032, doi:10.1029/2003JC002226.

——, P. Schaeffer, J.-M. Lemoine, and F. Hernandez, 2006: Estimation of the ocean mean dynamic topography through the combination of altimetric data, in-situ measurements and GRACE geoid: From global to regional studies. *Proc. GOCINA Int. Workshop,* Luxembourg, Centre Européan de Géodynamique et de Séismologie.

Rossby, T., 1996: The North Atlantic Current and surrounding waters: At the crossroads. *Rev. Geophys.,* **34,** 463–481.

——, D. Dorson, and J. Fontaine, 1986: The RAFOS system. *J. Atmos. Oceanic Technol.,* **3,** 672–679.

Saunders, P. M., 1994: The flux of overflow water through the Charlie-Gibbs Fracture Zone. *J. Geophys. Res.,* **99** (C3), 12 343–12 355.

Schott, F., L. Stramma, and J. Fischer, 1999: Interaction of the North Atlantic Current with the deep Charlie-Gibbs Fracture Zone throughflow. *Geophys. Res. Lett.,* **26,** 369–372.

Seale, R. C., 1981: The active part of Charlie-Gibbs Fracture Zone: A study using sonar and other geophysical techniques. *J. Geophys. Res.,* **86,** 243–262.

Smith, W. H. E., and D. T. Sandwell, 1997: Sea floor topography from satellite altimetry and ship depth soundings. *Science,* **277,** 1956–1962.

Sy, A., 1988: Investigation of large-scale circulation patterns in the central North Atlantic: The North Atlantic Current, the Azores Current, and the Mediterranean water plume in the area of the Mid-Atlantic Ridge. *Deep-Sea Res.,* **35,** 383–413.

——, U. Schauer, and J. Meincke, 1992: The North Atlantic Current and its associated hydrographic structure above and eastwards of the Mid-Atlantic Ridge. *Deep-Sea Res.,* **39,** 825–853.

White, M. A., and K. J. Heywood, 1995: Seasonal and interannual changes in the North Atlantic subpolar gyre from Geosat and TOPEX/POSEIDON altimetry. *J. Geophys. Res.,* **100,** 24 931–24 942.

Worthington, L. V., 1976: *On the North Atlantic Circulation*. Johns Hopkins University Press, 110 pp.